

CRISPR-based point-of-care diagnostics incorporating Cas9, Cas12, and Cas13 enzymes advanced for SARS-CoV-2 detection

Monika K. Verma¹ | Sanjana Roychowdhury¹ | Bidya Dhar Sahu² |
Awanish Mishra²  | Kalyan K. Sethi¹ 

¹Department of Medicinal Chemistry, National Institute of Pharmaceutical Education and Research (NIPER)—Guwahati, Changsari, Kamrup, Guwahati, Assam, India

²Department of Pharmacology and Toxicology, National Institute of Pharmaceutical Education and Research (NIPER)—Guwahati, Changsari, Kamrup, Guwahati, Assam, India

Correspondence

Awanish Mishra, Department of Pharmacology and Toxicology, National Institute of Pharmaceutical Education and Research (NIPER)—Guwahati, Sila Katamur (Halugurisuk), Changsari, Kamrup, Guwahati, Assam 781101, India.
Email: awanish@niperguwahati.in

Kalyan K. Sethi, Department of Medicinal Chemistry, National Institute of Pharmaceutical Education and Research (NIPER)—Guwahati, Sila Katamur (Halugurisuk), Changsari, Kamrup, Guwahati, Assam 781101, India.
Email: kalyan@niperguwahati.in and kalyansethi@gmail.com

Abstract

An outbreak of the novel beta coronavirus severe acute respiratory syndrome coronavirus 2 (SARS-CoV-2) first came to light in December 2019, which has unfolded rapidly and turned out to be a global pandemic. Early prognosis of viral contamination involves speedy intervention, disorder control, and good-sized management of the spread of disease. Reverse transcription-polymerase chain reaction, considered the gold standard test for detecting nucleic acids and pathogen diagnosis, provides high sensitivity and specificity. However, reliance on high-priced equipped kits, associated reagents, and skilled personnel slow down sickness detection. Lately, the improvement of clustered regularly interspaced short palindromic repeat (CRISPR)-Cas (CRISPR-associated protein)-based diagnostic systems has reshaped molecular diagnosis due to their low cost, simplicity, speed, efficiency, high sensitivity, specificity, and versatility, which is vital for accomplishing point-of-care diagnostics. We reviewed and summarized CRISPR-Cas-based point-of-care diagnostic strategies and research in these paintings while highlighting their characteristics and challenges for identifying SARS-CoV-2.

KEYWORDS

Cas9, Cas12, Cas13, CRISPR-Cas, RPA, RT-LAMP, SARS-CoV-2

1 | INTRODUCTION

A new pandemic outbreak first occurred in Wuhan, China, in December 2019, originating from a betacoronavirus, severe acute respiratory syndrome coronavirus 2 (SARS-CoV-2), causing mayhem among humanity, ensuing in more than three million deaths worldwide as well as millions of hospitalizations by the end of June 2021. A new strain of this illness has been named coronavirus disease 2019 (COVID-19) by the World Health Organization (WHO). The virulent SARS-CoV-2 causes a flu-like condition, and in some cases, severe acute respiratory syndrome (SARS).^[1] A person may contract the

disease either directly through droplets and hand-to-hand transmission or indirectly via contaminated objects and airborne contamination after encountering both symptomatic and asymptomatic patients.^[2]

These are the most significant single-stranded ribonucleic acid (ssRNA) viruses known in the deoxyribonucleic acid (DNA)-RNA genome, measuring 8.5–12 kDa in size.^[3] A viral genome comprises two sections, the 5' and 3' terminals. The 5'-terminal accounts for most of the genome, encoding a protein essential to viral replication, while the 3'-terminal encodes five structural proteins: the spike protein (S), an envelope protein (E), hemagglutinin esterase (HE),

membrane protein (M), and nucleocapsid protein (N).^[4,5] S protein plays a significant role in attaching viruses to their host cell membrane and facilitating the fusion of infected cells with uninfected ones adjacent to them. They are the major inducers of neutralizing antibodies during vaccination. The N protein forms an RNA complex that aids transcription and virulence. At the same time, the M protein serves as the predominant structural protein and is also responsible for the morphology of the virion envelope. One of the minor structural proteins, E proteins, is present in high levels inside infected cells as they replicate. In contrast, the HE protein controls the host specificity and receptor binding.^[3,6]

Rapid detection of COVID-19 via an accurate and fast method is essential to decrease the hazard of sickness spreading. With the aid of asymptomatic and symptomatic patients, the transmission chain of the SARS-CoV-2 virus could be broken, allowing diagnosis and prognosis to be tackled on a massive scale.^[7] Nevertheless, the increasing desire for rapid screening to understand whether individuals have COVID-19 contamination is a primary task in analysis. Currently, reverse transcription-polymerase chain reaction (RT-PCR) is considered the gold standard test for nucleic acid's qualitative and quantitative detection from the SARS-CoV-2 virus. Various challenges appear while performing RT-PCR testing on a large scale, including the need for expensive and complicated test devices and skilled laboratory employees' interpretation of the results. Thus, there is a pressing need for technologies, particularly point-of-care (POC) tests, to detect COVID-19 infections rapidly and accurately. Therefore, scientists have begun using clustered regularly interspaced short palindromic repeat (CRISPR)-Cas (CRISPR-associated protein), a technology initially designed for gene editing. Before going into details about CRISPR-Cas technology, we should first understand how RT-PCR detects COVID-19. Therefore, the following section provides an overview of the mechanism behind RT-PCR.

2 | AN OVERVIEW OF RT-PCR TESTING

Several countries considered RT-PCR-based testing the gold standard for the diagnosis of COVID-19.^[8] The COVID-19 RT-PCR test identifies RNA from the SARS-CoV-2 strain in the upper and lower respiratory tracts in real-time, using reverse transcription-polymerase chain reaction technology.^[9] Samples are taken through a nasopharyngeal or oropharyngeal swab. A swab is placed in the nostril and gently rolled forward into the nasopharynx to collect the secretions containing the virus. The swabs are immediately inoculated into sterile tubes filled with 2–3 ml of viral transport medium and protected from the degradation of viral nucleic acid by either keeping them at 2–8°C or –70°C for up to 72 h, based on the timing of testing.^[10,11] PCR, which is frequently used in molecular biology to rapidly copy large quantities of DNA fragments, is the standard method of COVID-19 testing.^[12] ssRNA genomes derived from COVID-19 are considerably large.^[13] Through reverse transcription, RNA molecules are turned into complementary DNA (cDNA)

sequences to be detected with PCR. A conventional PCR method can then be performed to amplify cDNA.^[14] The viral RNA should be extracted before performing the PCR. A wide range of kits for RNA purification is accessible, allowing rapid, convenient, and accurate isolation.

First, the sample is placed into a microcentrifuge tube to extract viral RNA. Afterward, a highly denaturing lysis buffer is added, usually composed of phenol and guanidine isothiocyanate.^[15] The lysis buffer is also expected to contain ribonuclease (RNase) inhibitors to prevent the degradation of viral RNA.^[16] With the lysis buffer added, the tube is pulse vortexed for 15 s, followed by a 10-min incubation at room temperature.^[17] The lysis buffer provides highly denaturing conditions under which the virus will be lysed. The lysed sample is loaded into a spin column and centrifuged for purification. It is a solid-phase extraction method that is performed using a silica matrix as the stationary phase. The silica gel membrane binds the RNA molecules under ideal pH and salt conditions while simultaneously retaining proteins and other contaminants.^[18] Spin columns are placed over clean collection tubes, and the filtrate is discarded after centrifugation. After the addition of wash buffer, the column goes back through centrifugation to force it through the membrane.^[19] As a result, the membrane is cleared of any remaining impurities, leaving only the RNA on the silica gel. An elution buffer is then added to the column after placing the washed sample in a clean microcentrifuge tube. Another centrifugation is performed, allowing the elution buffer to cross the membrane. Elution buffer cleans the viral RNA off the spin column, resulting in purified RNA free of proteins, inhibitors, and contaminants.^[20,21] Preparation of the reaction mixture for PCR amplification follows the extraction of viral RNA. RT-PCR master mix is used for this step, containing reverse transcriptase enzyme, nucleotides, forward primers, reverse primers, *Taq* (*Thermus aquaticus*) DNA polymerase TaqMan probe, and a concentrated buffer solution.^[22] The RNA template is then incorporated into the reaction mixture.

After pulse-vortexing the tube, the reaction mixture is loaded into a PCR plate, typically containing 96 wells, allowing multiple samples to be tested simultaneously.^[22,23] It is followed by placing the plate in a thermal cycler. COVID-19 is detected by quantitative PCR (qPCR), which amplifies specific target sequences within the *Rdrp* gene, the *E* gene, and the *N* gene.^[24] The primer and probe sequences determine which gene needs to be targeted. A primer is an oligonucleotide sequence about 18–24 bases long, while a probe has a length of 8–12 base pairs.^[25,26] COVID-19 detection requires the use of two or more primer pairs and probes targeted specifically at its nucleocapsid genes (*N* genes).^[27]

As shown in Figure 1, RT-PCR begins with a reverse transcription process. PCR reverse primers involve priming cDNA replication with a sequence that complements the viral RNA genome. Reverse transcriptase binds the DNA nucleotides on the 3' end, synthesizing a cDNA strand of the viral RNA.^[28] Depending on the primer, the target RNA, and the reverse transcriptase, this step will vary in temperature and duration. Once the extracted viral RNA and RT-PCR master mix were placed in a thermocycler, the PCR program was set

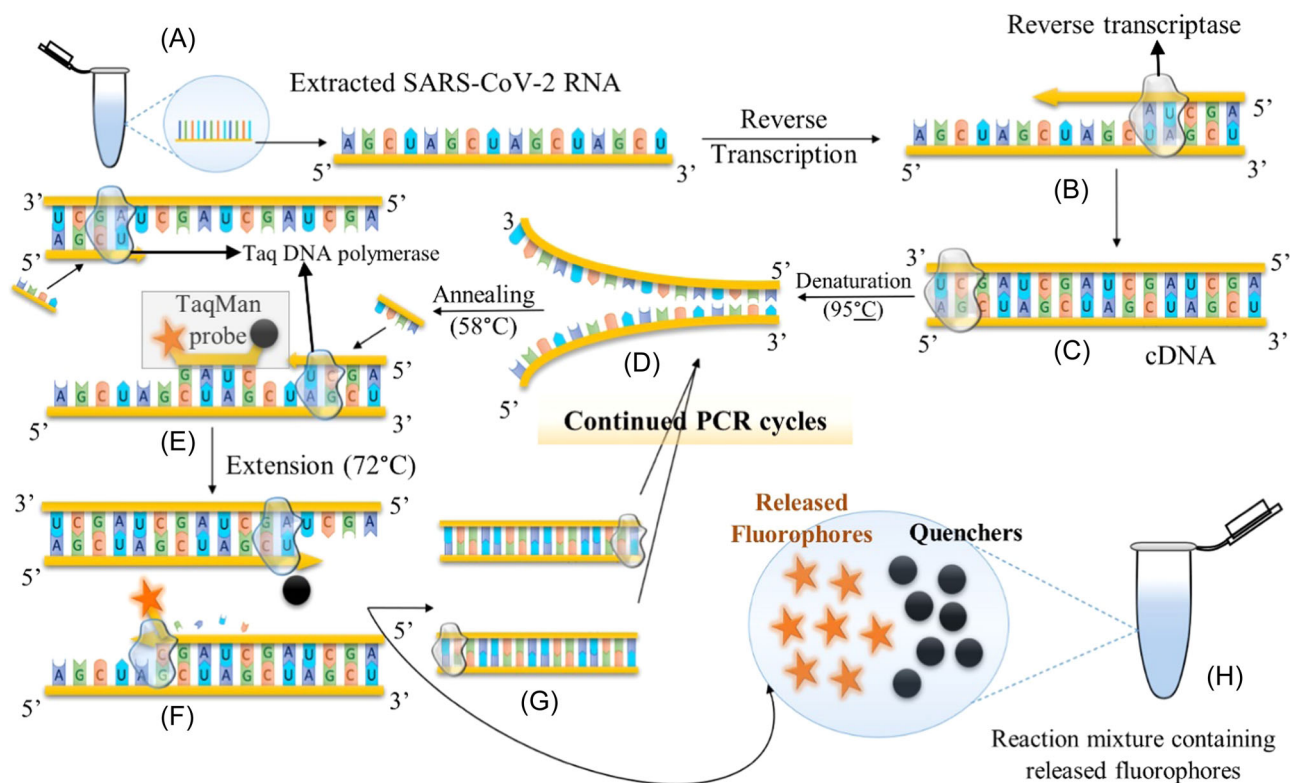


FIGURE 1 Mechanism of RT-PCR. (A) Isolation of viral RNA from samples collected; (B) reverse transcription of the viral RNA by reverse transcriptase enzyme; (C) synthesis of double-stranded DNA template (cDNA); (D) denaturation of cDNA at 95°C leading to the synthesis of ssDNA; (E) annealing—at 58°C, a fluorophore and quencher containing TaqMan probe, along with primers, anneals to specific sequences on the DNA strands; (F) extension—Taq DNA polymerase produces a new DNA strand at 72°C by adding free nucleotides and releasing the fluorophores and quenchers from the TaqMan probe by its 5′–3′ exonuclease activity; (G) amplification—multiple copies of cDNA are synthesized and then recycled through the PCR process; (H) in every PCR cycle, the release of fluorophores accumulates in the reaction mixture. cDNA, complementary DNA; RT-PCR, reverse transcription-polymerase chain reaction; ssDNA, single-stranded DNA.

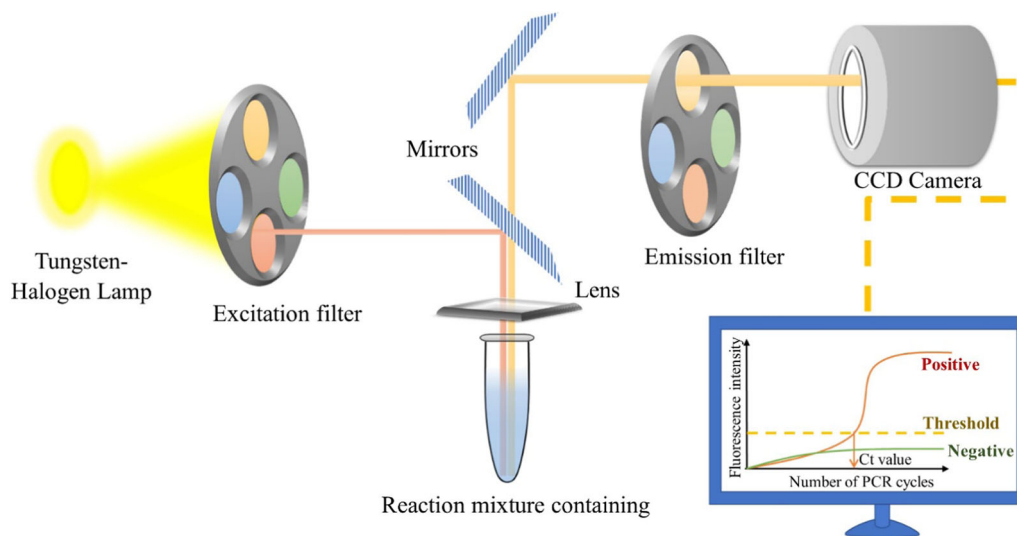


FIGURE 2 Detection and measurement of released fluorescence signal.

for denaturation (94°C), annealing (52–58°C), and extension (60–72°C) for target gene amplification. The denaturation process separates the double-stranded cDNA (ds-cDNA) from single-

stranded DNA (ssDNA) at 94°C. The primers and probes anneal to the template as the temperature drops between 52°C and 58°C.^[22] Taq DNA polymerase encounters the TaqMan probe while elongating

a new copy of DNA. A fluorophore is attached covalently at its 5' end to TaqMan oligonucleotide probe.^[29] The probe also includes a quencher at its 3' end. As the reporter is close to the quencher, its fluorescence cannot be observed. The extension step involves Taq DNA polymerase synthesizing new strands. The polymerase's 5'-3' exonuclease activity breaks down the TaqMan probe and the quencher releases the fluorophore, causing it to emit fluorescence.^[28,30] Increasing fluorescence intensity occurs with each cycle of PCR in a real-time manner as more fluorophores are released.

Figure 2 shows that the fluorescence signal is measured using a tungsten-halogen lamp, an excitation filter, mirrors, a lens, an emission filter, and a charge-coupled device (CCD) camera.^[31] A mirror reflects the filtered light from the lamp, which is then focused onto each well through a condensing lens. In the next step, fluorescence emitted from the wells is reflected off the mirror, transmitted through a filter, and detected by the CCD camera. The CCD camera detects the light from excited fluorophores with each PCR cycle, converting it to digital data.^[31,32] The amplification results are shown as C_t (cycle threshold) values. C_t value represents the quantity of target messenger RNA (mRNA) present in the sample. A lower C_t value corresponds to a higher copy number of the target. Hence, a low C_t value indicates a high viral load in COVID-19 infection cases. Globally, the C_t value for COVID-19 falls between 35 and 40.^[33,34] The tests are conducted in replicates to enhance their reliability, followed by their statistical significance assessment.

However, the limited supply of reagents, a long wait for results, and a labor-intensive procedure have caused many to consider alternative testing methods. Thus, diagnostic systems based entirely on CRISPR-Cas have been employed. CRISPR-Cas-based technology does not require a high-priced, complex system and detects SARS-CoV-2 within 1 h with sensitivity and specificity equivalent to standard PCR using fluorescence or lateral drift assay. Detailed information about CRISPR-Cas and its mechanism is provided in the next section.

3 | AN OVERVIEW OF CRISPR-CAS TECHNOLOGY AND ITS MECHANISMS

Like most tools in biotechnology and microbiology, CRISPR was first identified in the prokaryotic cells of *Escherichia coli* by Dr. Nakata's group.^[35] CRISPR has the potential to reshape the field of genetics because of its robustness compared to other existing tools. The name itself describes some of the main aspects of CRISPR. Short and Repeats are the words that describe it as short, identical repeats of DNA, usually 28–37 base pairs long but ranging from as little as 23–55 nucleotides (nt) in length. The word Palindromic depicts that the repeats use palindrome sequences to recognize specific sequences of DNA for transcription to make mRNA, resulting in tiny hairpin-like secondary structures. These repeats are regularly interspaced, that is, there are regular unique spacers in the middle of the repeats known as spacer DNA or CRISPR spacers ranging from 32 to 38 nt in size.^[36] In 1993, CRISPRs were primarily found in archaea,

especially in *Haloferax mediterranei*.^[37] Ten to forty percent of bacteria and the majority of archaea contain this system.^[38] In the early 2000s, scientists discovered that these spacer sequences exactly match the sequences of bacteriophages, archaeal viruses, and plasmids, demonstrating that CRISPR functions as an immune system.^[39] Additionally, scientists have identified that properly conserved genes have invariably been adjacent to CRISPR elements known as Cas (CRISPR-associated) genes.^[40] These Cas genes encode proteins or enzymes, such as DNA polymerases, helicases, and RecB-like nucleases.^[41]

The two main classes of CRISPR-Cas systems, Class 1 and Class 2, rely on the ability of effector Cas proteins to cleave foreign nucleic acids, further subdivided into six categories and over 30 subcategories. Studies and applications using the Class 2 system demonstrate that gene editing and genetic screening are more feasible with the Class 2 system, consisting of CRISPR-Cas Types II, V, and VI. The effector proteins for Types II, V, and VI are Cas9, Cas12, and Cas13, respectively.^[42,43] Defence initiated by CRISPR-Cas is divided into three phases (Figure 3). In the first stage, adaptation, new spacers are inserted from exogenous nucleic acids into the CRISPR locus.^[44]

CRISPR RNA (crRNA) biogenesis is the second phase of the system. In bacterial DNA, CRISPR repeats and spacers from the CRISPR locus are transcribed to produce single-chain RNA called precursor-CRISPR RNA (pre-crRNA).^[36] These long pre-crRNAs are then cleaved into 20-nt-long fragments called crRNA by Cas enzymes and associated factors in most systems.^[45,46] Hence, each crRNA contains complementary sequences derived from CRISPR repeats and viral genome sequences. Cas9, the effector protein of the Type II CRISPR-Cas system, performs double-stranded DNA break by utilizing two domains (HNH and RuvC), which are RNaseH like endonuclease domains responsible for cleaving complementary and noncomplementary sequences of the target DNA, respectively.^[46] Type II of CRISPR also involves fragments of trans-activating crRNA (tracrRNA) bound to CRISPR repeats on mRNA by an interconnecting loop. The complex formed by combining tracrRNA and crRNA is guide RNA (gRNA). RNase III enzymes are then used to cleave the loop.^[47] After the loop is cut, the "N"-any nucleobase, "GG"-2 guanine nucleobases (NGG) sequence of protospacer adjacent motif (PAM) site of the Cas9 protein is activated. The catalytic units cleave the DNA at specific locations, leaving the CRISPR repeat, the viral genome, and the tracrRNA in combination.^[48] The Type V system uses cas12 as its signature effector protein, a single crRNA-guide endonuclease.

Contrary to the blunt ends of Cas9, Cas12 uses a staggered double-stranded DNA break to cleave sequence-specific DNA with a 5' overhang via the RuvC and Nuc domain.^[49] Type VI systems contain only one effector protein, Cas13, interacting with crRNA, forming a guide crRNA that identifies a complementary RNA target. The target is cleaved by catalytic sites within the two preserved higher eukaryotes and prokaryotes nucleotide-binding (HEPN) domains. Modifications to HEPN domains can cause RNA-binding proteins to be inactive.^[50,51] The third and last stage, interference, involves targeting and cleaving foreign nucleic acids within the

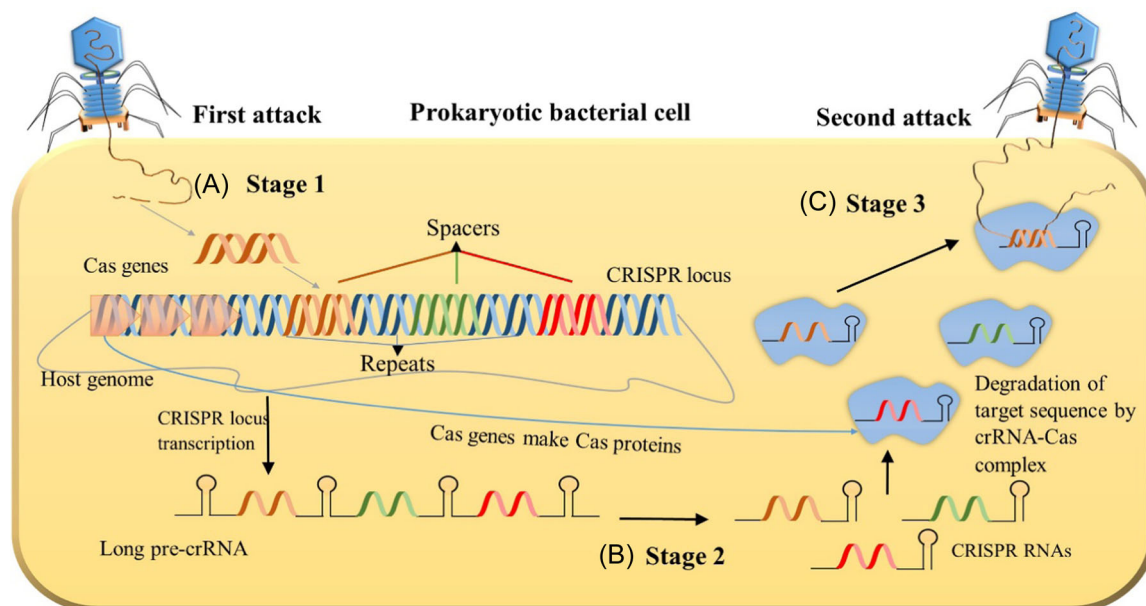


FIGURE 3 CRISPR–Cas mediated defense mechanism. (A) Adaptation or space acquisition: Introducing foreign nucleic acids into the CRISPR loci as new spacers; (B) crRNA biogenesis: Producing pre-crRNA transcripts by one of two strands of spacer DNA from the CRISPR locus, followed by cleavage into crRNAs; (C) interference: Integrating the crRNA with the Cas enzyme to form CRISPR–Cas complex, which recognizes and cleaves the viral genome when the same virus invades the cell again. Cas, CRISPR-associated proteins; CRISPR, clustered regularly interspaced short palindromic repeats; crRNA, CRISPR RNA.

protospacer sequence. The crRNAs direct respective Cas protein complexes to locate the corresponding protospacers to facilitate the degradation of their respective target sequences on the complementary virus or plasmid that match the spacers.^[52,53]

To summarize, when a bacteriophage attaches itself to the surface of a bacterial cell and injects its genome DNA, it will produce lots of bacteriophages that will eventually kill the cell. By using the CRISPR–Cas-mediated immune defense described above, the bacteriophage genome will be destroyed on the subsequent invasion, preventing it from increasing inside the bacterial cells, thus allowing them to protect themselves. Hence, the infection ends before it even begins. The ribonucleoprotein (RNP) complex formed with these crRNAs and Cas proteins guides these proteins to the specific region of the viral genome to be cleaved, thus serving the purpose of nucleic acid recognition of SARS-CoV-2 viruses.^[54] In this review, we will elaborate on the fundamental use of three proteins, mainly Cas9, Cas12, and Cas13, with CRISPR, as markers for SARS-CoV-2 detection.

3.1 | CRISPR–Cas9 system

Jennifer Doudna and Emmanuelle Charpentier discovered the CRISPR–Cas9 system while working with *Streptococcus pyogenes*. In 2020, the Nobel Prize in Chemistry was awarded to them to develop this revolutionary gene-editing tool.^[55] The Cas9 protein found in *Francisella novicida* (FnCas9) is among the largest orthologs of Cas9, and its interactions with DNA are primarily concentrated on the

5′-NGG-3′ PAM motif.^[56] The DNA interrogation mediated by CRISPR/FnCas9 followed by cleaving of both strands serves as a fast and accurate way to detect any single-nucleotide variant under the assumption that the DNA discrimination mechanism remains constant over the entire genome sequence. Azhar et al.^[57] named this framework FnCas9 Editor Linked Uniform Detection Assay (FELUDA). In association with the TATA group, the New Delhi-based CSIR-Institute of Genomics and Integrative Biology developed the FELUDA test.^[58] FELUDA is an example of a recently approved paper-based strip test to detect COVID-19 infection. In 2020, the Drugs Controller General of India and the Indian Council of Medical Research, New Delhi, India approved the FELUDA testing technology, which was later licensed to TATA Medical Diagnostics and is being marketed for use in a variety of diagnostic applications.^[59] FELUDA uses the same sampling technique as qPCR, in which samples are taken via oropharyngeal, nasopharyngeal swab, or saliva, followed by RNA extraction. Once RNA has been extracted, reverse transcription-polymerase chain reaction (RT-PCR) is carried out on a standard PCR machine instead of a 20-fold more expensive qPCR.^[60]

A single-step RT-PCR is followed by incubation of the amplified viral DNA with FELUDA mix, which contains deactivated FnCas9 (dFnCas9) protein and guide RNA.^[61] In reverse transcription, biotin-tagged primers are used. As a result, amplicons are biotin-labeled in PCR.^[62] The Cas9 RNP complex binds specifically to the 20 nt target sequence for determining if it carries the SARS-CoV-2 signature. Once it has located the signature, it moves along with the gold nanoparticles (NPs) in the paper strip. The gold NPs are mixed with the streptavidin protein, combining with the viral genome. In other

words, the gold NP-bound FELUDA complex is captured by interacting with streptavidin-biotin.^[63,64]

These NPs can recognize fluorescent amidite (FAM) (Figure 4). At the 3' end of the guide RNA, this FAM is bound to the RNP complex. In this manner, the NP initially captures the RNP complexes by adhering to the FAM label on the 3' end of guide RNA.^[64] In the presence of viral genomes, the test band will be colored. Unbound gold NPs are captured on the control band. Hence, negative samples will not have a band at the test region, whereas positive samples will have both test and control bands. FELUDA analyzes mostly S and N of the SARS-CoV-2 with its commercial kit. The limit of detection is 10 viral RNA copies/ μl . Lab tests show FELUDA to have an overall sensitivity and specificity of approximately 97% and 100%.^[62] The advantages of the FELUDA test include having a minimal technical expertise requirement and no expensive equipment requirement, making the test easy to administer at the point of care. The procedure takes between 60 and 75 min and costs about 500 INR, which is considerably low compared to deep sequencing.^[65] The authors added that FELUDA is compatible with conventional PCR, resulting in a reduced assay time of 45 min.^[57,66] With the combination of FELUDA and rapid variant assay (RAY), it is also possible to identify SARS-CoV-2 from other coronavirus strains, regardless of their minute genetic differences. With the use of

dFnCas9, RAY uses a high degree of specificity to identify point mismatches specifically and has the capability of differentiating among targets independently.^[67]

A disadvantage of this CRISPR-Cas9 based technique is the requirement for a thermal cycler, whereas the isothermal amplification method aids in improving POC diagnostic system, which is observed with the CRISPR-Cas12 system.

3.2 | CRISPR-Cas12 system

Cas12 and Cas13 are among the most effective CRISPR-Cas systems with excellent collateral cleavage activity toward ssDNA and RNA targets. Detecting nucleic acids using such collateral activity is highly specific and sensitive.^[68-71] SARS-CoV-2 detection methods based on CRISPR frequently use cas12 enzymes to recognize the viral sequence. CRISPR-Cas12 is viewed as an attractive alternative to Cas9 because of its unique features, such as its ability to target motifs that contain T-rich sequences and the absence of tracrRNA.^[72] The CRISPR-based diagnostic methods rely on a wide range of isothermal amplification techniques, such as loop-mediated isothermal amplification (LAMP) and recombinase polymerase amplification (RPA) enabling rapid, highly specific, and sensitive amplification of few

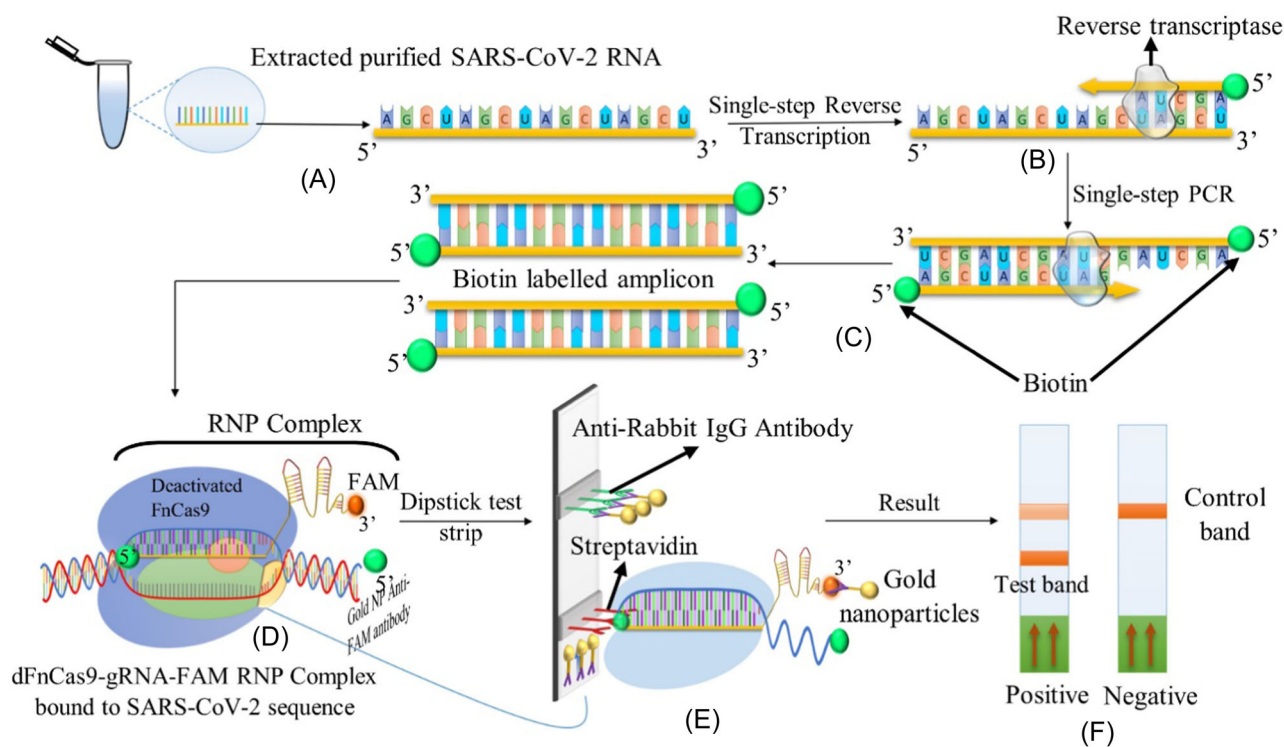


FIGURE 4 COVID-19 detection using CRISPR-Cas9 system. (A) Extraction of purified viral RNA; (B) synthesis of biotin-labeled cDNA templates by reverse transcriptase enzyme; (C) production of PCR amplicons with biotin-labeled primers; (D) insertion of target DNA sequence into dFnCas9-gRNA-FAM RNP complex; (E) specific identification of positive SARS-CoV-2 amplicons by dFnCas9 RNP complex; (F) visual analysis of positive and negative samples on dipstick test strips. Cas, CRISPR-associated proteins; CRISPR, clustered regularly interspaced short palindromic repeats; cDNA, complementary DNA; COVID-19, coronavirus disease 2019; FAM, fluorescent amidite; gDNA, guide DNA; RNP, ribonucleoprotein; SARS, severe acute respiratory syndrome.

copies of the target nucleic acid in a short period.^[73,74] Since these methods do not require thermocycling; they are ideal for low-cost POC diagnostic testing.

The DNA endonuclease-targeted CRISPR trans reporter (DETECTR), the device utilizes a reverse transcription-LAMP in conjunction with CRISPR-Cas12 to provide quick, accurate, and sensitive detection of SARS-CoV-2.^[75] Reverse transcription-LAMP and CRISPR-Cas12 reactions can be characterized as fast because they take less than 1 h. It is specific because it needs to identify and then cleave Sars-Cov-2 sequences using the cas12 enzyme. This system is portable and easy to use since only a simple system is required, and the colorimetric reaction and lateral flow assay results are easily interpreted. The following steps are undertaken in this method: reverse transcription amplification (RTA), Cas12a targeting and detection, and signal reading and interpretation.

3.2.1 | RTA

Reverse transcription-LAMP is a rapid and cost-effective alternative for testing SARS-CoV-2. This approach combines LAMP DNA-detection and reverse transcription, converting RNA into cDNA

before running the reaction.^[76] For example, SARS-CoV-2 and Ebola viruses can be detected using reverse transcription-LAMP.^[77] As opposed to PCR, reverse transcription-LAMP is not subject to the thermocycling step and typically takes place at 60–65°C temperature. This simple diagnostic test entails only heating and visual examination, but it is highly sensitive and simple, making it an excellent virus detection method.^[78] During reverse transcription-LAMP, viral RNA is extracted from swab samples and subjected to preamplification because it is challenging for CRISPR to detect targets in a reasonable time frame (less than an hour) when their concentration is extremely low (below 10 nM).^[79,80]

Four LAMP primers detect a specific sequence of cDNA. As illustrated in Figure 5, there are two inner primers—forward inner primer (FIP) and backward inner primer (BIP). These serve as the bases for *Bst* (*Bacillus stearothermophilus*) to copy the DNA template to new DNA. The outer primers, such as forward exterior primer (F3) and backward outer primer (B3), bind to the template strand and aid in reaction. In contrast to RT-PCR, the reverse transcription-LAMP procedure starts by generating DNA from the sample RNA. Reverse transcriptase, an enzyme produced by retroviruses, turns RNA into cDNA.^[81] A ssDNA copy is generated by reverse transcriptase with the help of an FIP primer. The F3 primer is also

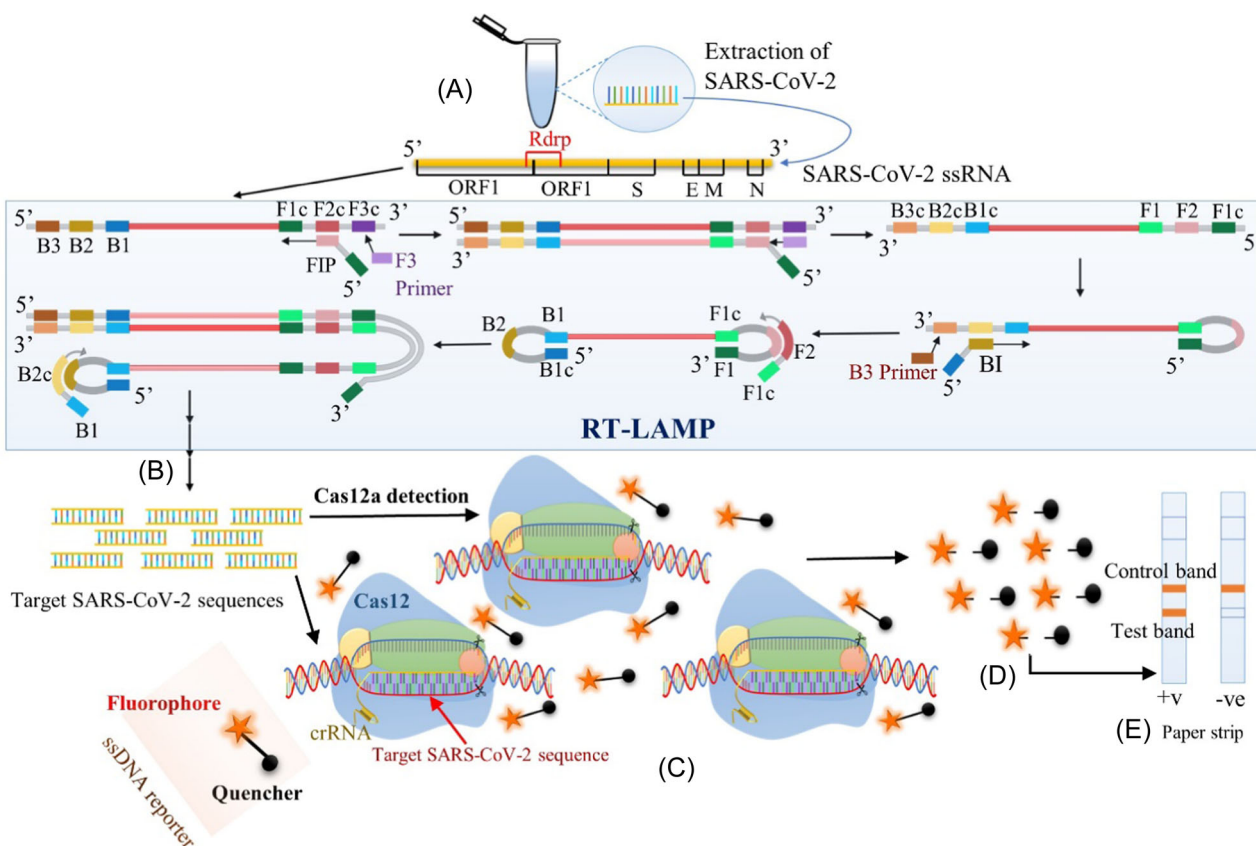


FIGURE 5 COVID-19 detection using CRISPR-Cas12a system. (A) Extraction of purified viral RNA; (B) synthesis of complementary DNA (cDNA) using RT-LAMP method; (C) recognition of viral RNA by CRISPR-Cas12a complex and cleavage of ssDNA reporter; (D) separation of fluorescent dyes and quenchers due to collateral cleavage; (E) visual interpretation of positive and negative samples on a paper strip. Cas, CRISPR-associated proteins; COVID-19, coronavirus disease 2019; CRISPR, clustered regularly interspaced short palindromic repeats; RT-LAMP, reverse transcription-loop-mediated isothermal amplification.

TABLE 1 List of a few modified methods using Cas12 enzymes, along with their advantages

| Cas type | System | Advantages | Time | Ref. |
|----------|-------------------|---|-----------|------|
| Cas12a | DETECTR | <ul style="list-style-type: none"> No thermocycling is required. Single-nucleotide specificity. No complex laboratory setup and easy to implement. Provide accurate results. Rapid turnaround time. | 30–40 min | [89] |
| Cas12b | STOPCovid | <ul style="list-style-type: none"> Easy, quick, to be performed at the POC. Sensitive and affordable. Comes with test components, and does not require extraction of RNA. | 1 h | [90] |
| Cas12a | CRISPR-FDS | This technique is sensitive, robust, fast, and feasible with available equipment. | ~50 min | [91] |
| Cas12a | AIOD-CRISPR | <ul style="list-style-type: none"> An intuitive, rapid, sensitive, and specific one-pot reaction without the need for separate preamplification or transferring of amplified products. Analyzing both DNA and RNA nucleic acids. Readily attainable in a single step. Single-molecule awareness. Robust performance. | 40 min | [92] |
| Cas12a | CRISPR/Cas12a-NER | <ul style="list-style-type: none"> Simple, convenient, precise. No special tools needed. Rapid and noticeable to the naked eye. | 45 min | [93] |

Abbreviations: AIOD, all-in-one dual; Cas, CRISPR-associated proteins; CRISPR, clustered regularly interspaced short palindromic repeats; DETECTR, DNA endonuclease-targeted CRISPR trans reporter; FDS, fluorescent detection system; NER, naked eye readout; POC, point-of-care; STOPCovid, specific high-sensitivity enzymatic reporter unlocking (SHERLOCK) testing in one pot.

bound to this side of the template strand, dislodging the earlier copies. This single-stranded displaced copy contains primers and RNA target. Primer sequences are designed with a region that binds to the DNA sequence, forming a loop. BIP primer is attached to the reverse end of the displaced strand to make double-stranded DNA, and Bst DNA polymerase uses it to make a complementary strand. This very same primer marks the beginning of this newly generated ssDNA molecule, thereby dislodging it.^[82] Using the freshly designed single strand, the LAMP cycling amplification can be initiated. Due to the folding and self-binding of the two loops, ssDNA has a dumbbell-shaped structure.^[83]

DNA polymerase with both FIP and BIP continues to amplify this strand, prolonging the LAMP reaction product. Depending on the type of primer used, this cycle may begin on either the forward or the reverse side of the strand. Once the strand commences the process of this cycle, the elongation step results in the synthesis of self-primed DNA. It takes nearly an hour to amplify this RNA between 60°C and 65°C so that a wide range of amplicons are produced after these steps.^[74]

3.2.2 | Cas12a targeting and detection

The cas12a/crRNA complex consists of guide RNA with a length of 40–44 base pairs, which includes a constant loop-stem region of 20-nt-long base pairs with a 20–24-nt protospacer region. This protospacer region should be designed based on the target

sequence.^[74] The loop domain is specific to Cas12a proteins. CRISPR-RNAs used in conjunction with cas12a to identify the PAM sequence, TTTV, where V represents A, C, or G of the SARS-CoV-2 genome.^[84] crRNA binds to the opposite DNA sequence of the PAM sequence. Therefore, the protospacer region must be exactly 20–24 bases long after the PAM region.^[85] The target amplicons will be incorporated into the Cas12a/crRNA complex. The Cas12a would then cleave adjacent nontarget reporters as collateral damage upon binding to the specific RNA target. Reporters are typically ssDNA with either the fluorophore quencher or the fluorophore biotin label attached.^[86]

3.2.3 | Signal readout and interpretation

An ssDNA reporter is trans-cleaved, and then the resulting signals are detected either with fluorescence-based reactions or individually with a colorimetric lateral flow reaction.^[87] Since Cas12a and reverse transcription-LAMP are performed separately, DETECTR is susceptible to contamination despite its high accuracy. Thus, there is a risk of receiving false-positive results. Scientists worked on a thermostable Cas12b derived from *Alicyclobacillus acidophilus* (AapCas12b) to address this problem in conjunction with reverse transcription-LAMP detection.^[88] Specific high-sensitivity enzymatic reporter unlocking (SHERLOCK) testing in one pot (STOPCovid) is a method

that yielded results from a single pot and a single temperature. Using a single-tube assay, SARS-CoV-2 could be detected more efficiently while reducing the risk of postamplification contamination.^[87] Numerous other optimized systems or combinatorial processes have also been observed with cas12. A few examples are listed below, highlighting their advantages (Table 1).

3.3 | CRISPR–Cas13 system

The CRISPR–Cas Type VI system uses RNA-guided gene-editing technology to grant prokaryotes immunity against RNA, belonging to Class 2.^[50] As of now, all CRISPR–Cas-based Type VI systems use just one effector protein, called Cas13a, which was formerly referred to as the C2c2 CRISPR–Cas complex.^[50,94] This Cas13a protein belongs to different Cas13 families, which are used to construct various subtypes of Cas13 (A–D).^[95–97] Various Cas13 variants can target and engineer transcriptomes with different degrees of effectiveness. Cas13a from *Leptotrichia wadei* (LwaCas13a) achieves a more powerful RNA-targeting effect but requires integration with a stabilizer for efficient interference activity.^[97] Researchers have discovered a variant of Cas13b found in *Prevotella* sp. P5–125 (PspCas13b) targets RNA better than the LwaCas13a protein in mammalian cells, and its activity is not affected by stabilizing proteins.^[96] There is yet another Cas13d subtype (Type VI-D) that shares little sequence homology with known endo-RNase-related Cas13 effectors.^[98] A notable feature of Cas13d is that it has a significantly reduced mass than all previously reported Cas13 endo-RNases.^[98] As a result, these Cas13 effector proteins can be used in RNA-targeting applications, including knocking down RNA, seeing its activity, editing it or splicing it, and delivering viruses.^[96,97,99,100]

CRISPR–Cas13 structures are composed of two functional elements. (I) RNA-guided and single-effector RNase cas13, encoding an RNase action brought about by its two HEPN. (II) A pre-crRNA, consisting of 64–66-nt-long sequence, identifies mature crRNAs of 24–30 nt sequence at the targeted RNA, is characterized by a protospacer flanking site motif.^[94,101,102] Upon activation through target-specific RNA, these systems exhibit collateral promiscuity and degrade RNA transcripts nonspecifically.^[50,99]

As part of the CRISPR–Cas13 system, crRNA is formed using a target spacer sequence and an attached stem-loop, direct repeat (DR).^[96] Cas13 then locates the DR and directs the crRNA to set up an exact match between the spacers and complementarily sequenced sample RNA.^[50] Contrary to Cas9, Cas13 fragments the terminal part of a spacer-paired RNA target sequence.^[50] Cleavage by Cas13 is sequence-specific, which can happen even if the RNA is far from the target sequence, although Cas13 can only cut ssRNA.^[50] In addition, Cas13 cannot detect mismatches between two base pairs in RNA–spacer pairings but can recognize mismatches between single base pairs. The Cas13 protein can also trans (collateral) cleavage activity, that is, degradation of surrounding ssRNA not targeted by the enzyme. This collateral cleavage activity is highly influenced by target cleavage.^[50] The direction of collateral cleavage is determined

by the preference for specific dinucleotides, which vary considerably among Cas13 orthologs.^[98] Collateral cleavage ability of Cas13 is a crucial element of Cas13 diagnostic testing.

A CRISPR–Cas13 diagnostic test incorporates a detection mix made up of Cas13a, RNA extracted from the sample, custom crRNA, and reporter RNA (RNA sensor) with a fluorophore and quencher.^[99] A sample RNA containing the target sequence will cause Cas13 to cleave the RNA sensor, releasing the fluorescent indicator collaterally.^[99] Thus, fluorescence is an output to show whether the target is present. This fluorescence level can calculate the amount of target present in the sample.^[98,103–106] The test is called SHERLOCK.^[99]

As a molecular biological detection technology, SHERLOCK was initially used for detecting nucleic acids rapidly in human health applications. Specifically, this method was used to identify several Zika and Dengue virus strains, along with other potentially infectious bacteria.^[99,103] To detect SARS-CoV-2 viral RNA, the current approach uses SHERLOCK as a CRISPR-based diagnostic platform. When a Cas13 enzyme combines with a virus targeting RNA, the virus will be cleaved, resulting in subsequent RNase activity.^[50,87] SHERLOCK is a two-step process. After nucleic acid purification, it is amplified by RPA (for DNA) and reverse transcription-RPA (for RNA). Following the amplification of the nucleic acids, it is transcribed by T7 RNA polymerase, which again produces RNA. The second step involves adding the amplified RNA into the CRISPR–Cas13 target identification reaction.^[98] Upon binding to targeted viral RNA, cas13 complexed with crRNA activates the cleavage activity, causing RNA sensor degradation, resulting in the production of a fluorescent dye, allowing the detection of that virus. Single targets can be detected using a commercial lateral flow strip.^[104]

In this case, detection is performed by using a lateral flow readout. The detection method based on lateral flow uses an RNA sensor. The sensor consists of a few nucleotides in the middle, followed by FAM and biotin at the ends. Streptavidin binds to biotin in the lateral flow strips, encapsulating the whole probe. An antibody labeled with FAM-specific gold NPs will attach to the fluorophore end of the RNA sensor and create a dark purple color at the top. Upon cleavage of RNA reporters due to a target and collateral activity, gold NP-labeled antibodies migrate to secondary anti-species antibodies, taking up all the antibodies to form dark purple that indicates the presence of targets in each clinical sample. Strips show one line for noninfected patients but two lines for those with the disease, as shown in Figure 6. Overall, one can read results as quickly as a pregnancy test, and no additional instruments are needed.

Recent studies have found that the SHERLOCK system is 96% specific and 100% effective for identifying SARS-CoV-2 in COVID-19 samples.^[105] By optimizing the RPA step of SHERLOCK, detection is made more accurate, and sensitivity is improved. A modified version of SHERLOCK allows amplification without PCR, ensuring 100% specificity and 100% sensitivity. Furthermore, SHERLOCK is very convenient due to its speed. Following RPA and T7-RT, the first steps are usually completed within 30–45 min. As a second step, the detection setup takes less than 15 min, and the fluorescence and lateral flow results are delivered after 1 and 1.5 h, respectively.^[87]

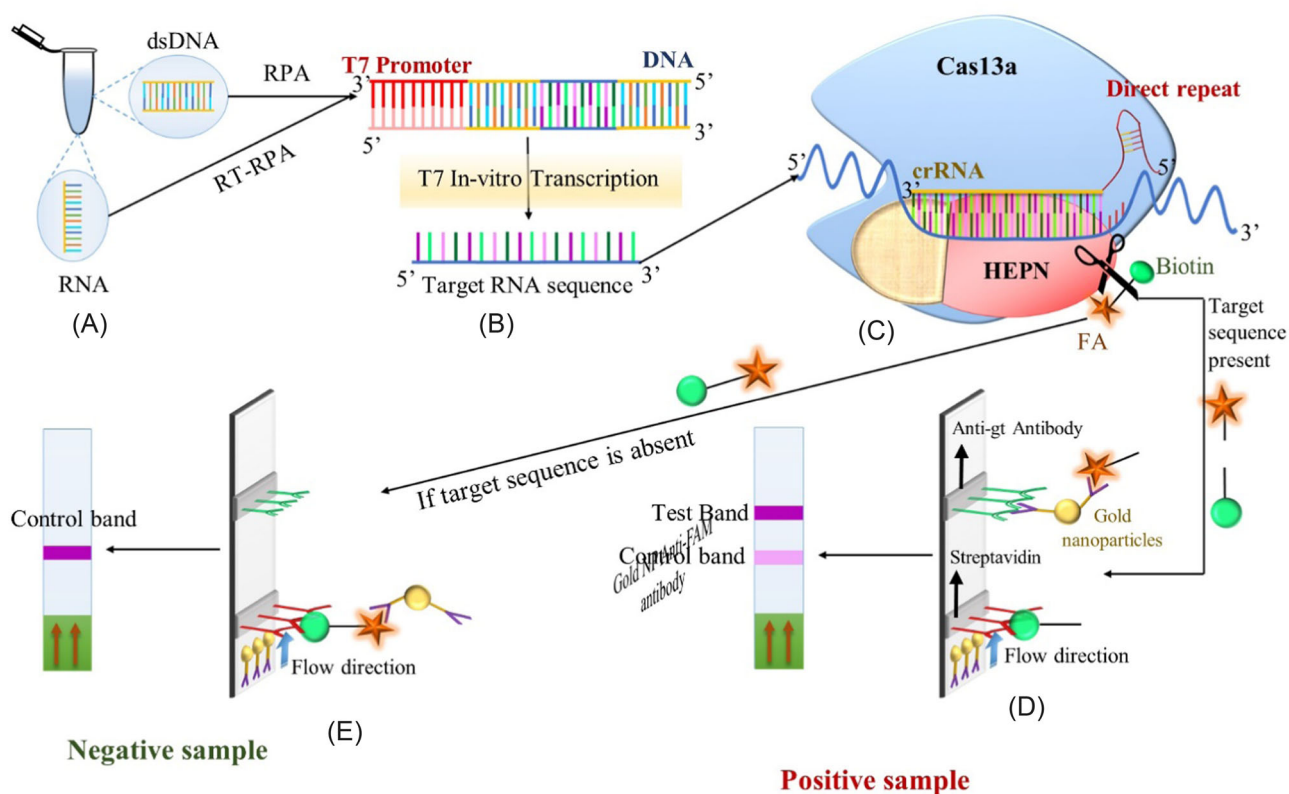


FIGURE 6 COVID-19 detection using CRISPR–Cas13a system. (A) Extraction of purified viral DNA or RNA; (B) formation of target RNA sequence from amplified DNA by T7 in vitro transcription; (C) recognition and collateral cleavage of RNA sensor by HEPN domain; (D, E) visual readout of positive and negative samples via lateral flow strip. Cas, CRISPR-associated proteins; COVID-19, coronavirus disease 2019; CRISPR, clustered regularly interspaced short palindromic repeats; HEPN, higher eukaryotes and prokaryotes nucleotide-binding.

Thus, the entire SHERLOCK is completed in about 2 h. A typical SHERLOCK procedure is to amplify a target RNA and then detect SARS-CoV-2 using CRISPR nucleic acid detection.^[87] Each of these processing steps makes SHERLOCK a complex diagnostic platform because RNA extraction and multiple liquid handling techniques increase the risk of cross-contamination.^[106]

One of these approaches was developed by Myhrvold et al.^[103] By bypassing the need for nucleic acid extraction, Myhrvold et al.^[103] established a method that releases viral genomes directly from the clinical sample to be protected against degradation. This method is known as Heating Unextracted Diagnostic Samples to Obliterate Nucleases (HUDSON). The HUDSON system successfully inactivates the RNAses in body fluids through chemical and heat treatments. The rupture of the viral envelope releases nucleic acids and lyses the viral particles.^[103] Hudson's approach permits the indirect incorporation of biological samples directly into the mixing reaction of isothermal amplification without diluting or purifying and without interfering with subsequent amplification.^[103] Consequently, a laboratory setting and appropriately trained staff are not mandatory for this protocol.^[99,103] Based on this approach, Adrizti-Sanz and fellow researchers combined HUDSON with CRISPR-based programmability to design SHINE (SHERLOCK and HUDSON Integration to Navigate Epidemics). This portable diagnostic approach can detect target viral RNA immediately from unextracted clinical specimens using minimal equipment.^[107]

Over the previous method, this method has three advantages. To begin with, the two-step SHERLOCK method was combined into one. Second, the HUDSON was used in conjunction with the SHERLOCK detection method. Last, the fluorescence signal was evaluated using a smartphone application.^[103] Fluorescence readout in the tube. The smartphone application has made SHINE a scalable, high-throughput testing device and allows automated data analysis. Therefore, this platform can provide POC diagnostic tests for SARS-COV-2 without compromising sensitivity or specificity by reducing the need for specialized personnel, infrastructure, and time.

Likewise, many more methods were developed such as CREST (Cas13-based, Rugged, Equitable, Scalable Testing), SENSR (Sensitive Enzymatic Nucleic-acid Sequence Reporter), CARMEN-(Combinatorial Arrayed Reactions for Multiplexed Evaluation of Nucleic acids), to eliminate all the obstacles on our way to achieve POC Diagnostics.^[108–110]

4 | CONCLUSION AND FUTURE PROSPECTIVE

For the unconventional SARS-CoV-2 to be controlled, commercialized diagnostic tests are necessary to detect the infection early, confirm its identity, and monitor the patients. Currently, the gold standard of

diagnosis for COVID-19 is qPCR. However, qPCR can only be performed in laboratories since a highly specialized system and skilled personnel are required. Additionally, it can sometimes deliver false results. Therefore, there is a pressing need for a fast, affordable, and accurate diagnostic check that can be used at the point of care for viral detection and disease monitoring. Recent developments have resulted in new methods to detect nucleic acids and infectious agents based on CRISPR systems linked mainly to Cas9, Cas12, and Cas13 enzymes.^[42,111] COVID-19 can be managed with the design of a therapeutic drug based on a similar approach as the CRISPR–Cas13 system, which aims at the SARS-CoV-2 ssRNA genome. A variety of methods based on the CRISPR–Cas13 system have been tested and proposed by researchers to counteract continuously mutating variants of the virus.^[112–116] Moreover, the scientific community has also discussed the possibility of using these systems for molecular diagnostics.^[104,117–120] By utilizing these techniques, diagnostic structures can be accurately established in a shorter amount of time, allowing for high levels of sensitivity and specificity without complicated instruments. Two studies have demonstrated that CRISPR-based techniques have confirmed the presence of the SARS-CoV-2 genome that qPCR has rejected; these results have been established with next-generation sequencing or computerized tomography scans.^[121–123]

Although the RP-PCR technique remains the gold standard for diagnosis of COVID-19 (qualitative and quantitative analyses) and are economical, the development of the CRISPR–Cas system for COVID-19 diagnosis would provide a quick qualitative diagnosis at an early stage of the disease with great precision and accuracy. Considering suitable logistics their utility and application may be enhanced. Aside from COVID-19, these methods can be used to combat various pathogens, viruses, and fungi, regardless of their availability, that threatens humans' health, agriculture, and food supply. CRISPR is a step in the right direction toward treating the current pandemic and being a basis for diagnostics and testing.

ACKNOWLEDGMENTS

The authors would like to acknowledge Dr. U. S. N. Murty, Director, NIPER-Guwahati for his constant support and encouragement.

CONFLICT OF INTEREST

The authors declare no conflict of interest.

DATA AVAILABILITY STATEMENT

Data sharing is not applicable to this article as no datasets were generated or analyzed during the current study.

ORCID

Awanish Mishra  <http://orcid.org/0000-0001-7863-5581>

Kalyan K. Sethi  <http://orcid.org/0000-0002-7627-0053>

REFERENCES

- [1] W. J. Wiersinga, A. Rhodes, A. C. Cheng, S. J. Peacock, H. C. Prescott, *JAMA* **2020**, 324, 782. <https://doi.org/10.1001/jama.2020.12839>
- [2] F. Wu, S. Zhao, B. Yu, Y. M. Chen, W. Wang, Z. G. Song, Y. Hu, Z. W. Tao, J. H. Tian, Y. Y. Pei, M. L. Yuan, Y. L. Zhang, F. H. Dai, Y. Liu, Q. M. Wang, J. J. Zheng, L. Xu, E. C. Holmes, Y. Z. Zhang, *Nature* **2020**, 579(7798), 265. <https://doi.org/10.1038/s41586-020-2008-3>
- [3] L. van der Hoek, K. Pyrc, M. F. Jebbink, W. Vermeulen-Oost, R. J. M. Berkhout, K. C. Wolthers, P. M. E. Wertheim-van Dillen, J. Kaandorp, J. Spaargaren, B. Berkhout, *Nat. Med.* **2004**, 10(4), 368. <https://doi.org/10.1038/nm1024>
- [4] D. R. Beniac, A. Andonov, E. Grudski, T. F. Booth, *Nat. Struct. Mol. Biol.* **2006**, 13(8), 751. <https://doi.org/10.1038/nsmb1123>
- [5] B. Delmas, H. Laude, *J. Virol.* **1990**, 64(11), 5367. <https://doi.org/10.1128/JVI.64.11.5367-5375.1990>
- [6] J. Armstrong, H. Neimann, S. Smekens, P. Rottier, G. Warren, *Nature* **1984**, 308(5961), 751. <https://doi.org/10.1038/308751a0>
- [7] V. J. Munster, M. Koopmans, N. van Doremalen, D. van Riel, E. de Wit, *N. Engl. J. Med.* **2020**, 382(8), 692. <https://doi.org/10.1056/nejmp2000929>
- [8] L. J. Carter, L. V. Garner, J. W. Smoot, Y. Li, Q. Zhou, C. J. Saveson, J. M. Sasso, A. C. Gregg, D. J. Soares, T. R. Beskid, S. R. Jervey, C. Liu, *ACS Cent. Sci.* **2020**, 6(5), 591. <https://doi.org/10.1021/acscentsci.0c00501>
- [9] B. Krueger, *COVID-19 RT-PCR Test—Letter of Authorization*, FDA—US Food and Drug Administration, Silver Spring, MD **2021**.
- [10] Centers for Disease Control and Prevention, *Interim Guidelines for Collecting and Handling of Clinical Specimens for COVID-19 Testing*, Centers for Disease Control and Prevention, Atlanta, GA **2020**.
- [11] K. Locher, B. Velapatino, M. Caza, L. Li, C. Porter, M. Charles, *J. Clin. Microbiol.* **2021**, 59(5), <https://doi.org/10.1128/JCM.01562-20>
- [12] D. Caetano-Anollés, *Brenner's Encyclopedia of Genetics*, 2nd ed., Elsevier Inc., Amsterdam **2013**, p. 392. <https://doi.org/10.1016/B978-0-12-374984-0.01186-4>
- [13] K. King, *What Causes COVID-19? A Virus Causes COVID-19, So What is a Virus?*, McCann Health Medical Communications, San Francisco, CA **2020**.
- [14] T. W. Myers, D. H. Gelfand, *Biochemistry* **1991**, 30(31), 7661. <https://doi.org/10.1021/bi00245a001>
- [15] P. Chomczynski, N. Sacchi, *Anal. Biochem.* **1987**, 162(1), 156. [https://doi.org/10.1016/0003-2697\(87\)90021-2](https://doi.org/10.1016/0003-2697(87)90021-2)
- [16] X. Wang, B. Teferedegne, K. Shatzkes, W. Tu, H. Murata, *Anal. Biochem.* **2016**, 513, 21. <https://doi.org/10.1016/j.ab.2016.08.011>
- [17] J. M. Thomas, K. M. Bryson, J. L. Meier, *Methods in Enzymology*, Vol. 621, Academic Press Inc., New York **2019**, p. 31. <https://doi.org/10.1016/bs.mie.2019.02.022>
- [18] K. A. Hagan, W. L. Meier, J. P. Ferrance, J. P. Landers, *Anal. Chem.* **2009**, 81(13), 5249. <https://doi.org/10.1021/ac900820z>
- [19] T. G. W. Graham, C. D. Darzacq, G. M. Dailey, X. H. Nguyenla, E. Dis, van M. N. Esbin, A. Abidi, S. A. Stanley, X. Darzacq, R. Tjian, *PLoS One* **2021**, 16(2), e0246647. <https://doi.org/10.1371/journal.pone.0246647>
- [20] World Health Organisation, *Laboratory Testing for Coronavirus Disease (COVID-19) in Suspected Human Cases*, World Health Organisation, Geneva **2020**.
- [21] N. Gupta, V. Potdar, I. Praharaaj, S. Giri, G. Sapkal, P. Yadav, M. Choudhary, L. Dar, A. Sugunan, H. Kaur, A. Munivenkatappa, J. Shastri, K. Kaveri, S. Dutta, B. Malhotra, A. Jain, K. Nagamani, G. Shantala, S. Raut, M. Vegad, A. Sharma, A. Choudhary, M. Brijwal, A. Balakrishnan, J. Manjunatha, M. Pathak, S. Srinivasan, H. Banu, H. Sharma, P. Jain, P. Sunita, R. Ambica, B. Fageria, D. Patel, G. Rajbongshi, N. Vijay, J. Narayan, N. Aggarwal, A. Nagar, R. Gangakhedkar, P. Abraham, *Indian*

- J. Med. Res.* **2020**, *151* (2,3), 216. https://doi.org/10.4103/ijmr.IJMR_594_20
- [22] T. C. Lorenz, *J. Vis. Exp.* **2012**, 63, e3998. <https://doi.org/10.3791/3998>
- [23] Y. Mo, R. Wan, Q. Zhang, *Methods in Molecular Biology* **2012**, 926, 99. https://doi.org/10.1007/978-1-62703-002-1_7
- [24] F. Cui, H. S. Zhou, *Biosens. Bioelectron.* **2020**, 165, 112349. <https://doi.org/10.1016/j.bios.2020.112349>
- [25] C. W. Dieffenbach, T. M. Lowe, G. S. Dveksler, *Genome Res.* **1993**, 3(3), <https://doi.org/10.1101/gr.3.3.S30>
- [26] N. J. Haslam, N. E. Whiteford, G. Weber, A. Prügel-Bennett, J. W. Essex, C. Neylon, *PLoS One* **2008**, 3(6), 2500. <https://doi.org/10.1371/journal.pone.0002500>
- [27] Z. Zhang, Y. Zhou, Y. Zhang, Y. Guo, S. Tao, Z. Li, Q. Zhang, J. Cheng, *Microarrays Clin. Diagn.* **2005**, 114, 59. <https://doi.org/10.1385/1-59259-923-0-59>
- [28] P. M. Holland, R. D. Abramson, R. Watson, D. H. Gelfand, *Proc. Natl. Acad. Sci.* **1991**, 88(16), 7276. <https://doi.org/10.1073/pnas.88.16.7276>
- [29] S. Shahi, S. Zununi Vahed, N. Fathi, S. Sharifi, *Int. J. Biol. Macromol.* **2018**, 117, 983–992. <https://doi.org/10.1016/j.ijbiomac.2018.05.085>
- [30] K. J. Livak, S. J. Flood, J. Marmaro, W. Giusti, K. Deetz, *Genome Res.* **1995**, 4(6), 357. <https://doi.org/10.1101/gr.4.6.357>
- [31] D. J. Webb, C. M. Brown, *Methods in Molecular Biology*, Vol. 931 (Ed: N. J. Clifton), Humana Press, Totowa, NJ **2012**, p. 29. https://doi.org/10.1007/978-1-62703-056-4_2
- [32] S. Dunst, P. Tomancak, *Genetics* **2019**, 211(1), 15. <https://doi.org/10.1534/genetics.118.300227>
- [33] K. J. Livak, T. D. Schmittgen, *Methods* **2001**, 25(4), 402. <https://doi.org/10.1006/meth.2001.1262>
- [34] S. N. Rao, D. Manissero, V. R. Steele, J. Pareja, *Infect. Dis. Ther.* **2020**, 9(3), 573. <https://doi.org/10.6084/m9.figshare.12668408>
- [35] Y. Ishino, H. Shinagawa, K. Makino, M. Amemura, A. Nakata, *J. Bacteriol.* **1987**, 169(12), 5429. <https://doi.org/10.1128/jb.169.12.5429-5433.1987>
- [36] R. Barrangou, L. A. Marraffini, *Mol. Cell* **2014**, 54(2), 234. <https://doi.org/10.1016/j.molcel.2014.03.011>
- [37] F. J. M. Mojica, G. Juez, F. Rodriguez-Valera, *Mol. Microbiol.* **1993**, 9(3), 613. <https://doi.org/10.1111/j.1365-2958.1993.tb01721.x>
- [38] D. Burstein, C. L. Sun, C. T. Brown, I. Sharon, K. Anantharaman, A. J. Probst, B. C. Thomas, J. F. Banfield, *Nat. Commun.* **2016**, 7, 10613. <https://doi.org/10.1038/ncomms10613>
- [39] Y. Ishino, M. Krupovic, P. Forterre, *J. Bacteriol.* **2018**, 200(7), e00580. <https://doi.org/10.1128/JB.00580-17>
- [40] R. Jansen, J. D. A. van Embden, W. Gaastra, L. M. Schouls, *Mol. Microbiol.* **2002**, 43(6), 1565. <https://doi.org/10.1046/j.1365-2958.2002.02839.x>
- [41] T. Sinkunas, G. Gasiunas, C. Fremaux, R. Barrangou, P. Horvath, V. Siksnys, *EMBO J.* **2011**, 30(7), 1335. <https://doi.org/10.1038/emboj.2011.41>
- [42] K. S. Makarova, Y. I. Wolf, O. S. Alkhnbashi, F. Costa, S. A. Shah, S. J. Saunders, R. Barrangou, S. J. J. Brouns, E. Charpentier, D. H. Haft, P. Horvath, S. Moineau, F. J. M. Mojica, R. M. Terns, M. P. Terns, M. F. White, A. F. Yakunin, R. A. Garrett, J. van der Oost, R. Backofen, E. V. Koonin, *Nat. Rev. Microbiol.* **2015**, 13(11), 722. <https://doi.org/10.1038/nrmicro3569>
- [43] E. V. Koonin, K. S. Makarova, F. Zhang, *Curr. Opin. Microbiol.* **2017**, 37, 67. <https://doi.org/10.1016/j.mib.2017.05.008>
- [44] S. A. Jackson, R. E. McKenzie, R. D. Fagerlund, S. N. Kieper, P. C. Fineran, S. J. J. Brouns, *Science* **2017**, 356(6333), eaal5056. <https://doi.org/10.1126/science.aal5056>
- [45] L. A. Marraffini, E. J. Sontheimer, *Nat. Rev. Genet.* **2010**, 11, 181. <https://doi.org/10.1038/nrg2749>
- [46] M. Jinek, K. Chylinski, I. Fonfara, M. Hauer, J. A. Doudna, E. Charpentier, *Science* **2012**, 337(6096), 816. <https://doi.org/10.1126/science.1225829>
- [47] E. Deltcheva, K. Chylinski, C. M. Sharma, K. Gonzales, Y. Chao, Z. A. Pirzada, M. R. Eckert, J. Vogel, E. Charpentier, *Nature* **2011**, 471(7340), 602. <https://doi.org/10.1038/nature09886>
- [48] Y. Wei, R. M. Terns, M. P. Terns, *Genes Dev.* **2015**, 29(4), 356. <https://doi.org/10.1101/gad.257550.114>
- [49] B. Zetsche, J. S. Gootenberg, O. O. Abudayyeh, I. M. Slaymaker, K. S. Makarova, P. Essletzbichler, S. E. Volz, J. Joung, J. van der Oost, A. Regev, E. V. Koonin, F. Zhang, *Cell* **2015**, 163(3), 759. <https://doi.org/10.1016/j.cell.2015.09.038>
- [50] O. O. Abudayyeh, J. S. Gootenberg, S. Konermann, J. Joung, I. M. Slaymaker, D. B. T. Cox, S. Shmakov, K. S. Makarova, E. Semenova, L. Minakhin, K. Severinov, A. Regev, E. S. Lander, E. V. Koonin, F. Zhang, *Science* **2016**, 353(6299), 5573. <https://doi.org/10.1126/science.aaf5573>
- [51] A. East-Seletsky, M. R. O'Connell, D. Burstein, G. J. Knott, J. A. Doudna, *Mol. Cell* **2017**, 66(3), 373. <https://doi.org/10.1016/j.molcel.2017.04.008>
- [52] J. E. Garneau, M. È. Dupuis, M. Villion, D. A. Romero, R. Barrangou, P. Boyaval, C. Fremaux, P. Horvath, A. H. Magadán, S. Moineau, *Nature* **2010**, 468(7320), 67. <https://doi.org/10.1038/nature09523>
- [53] E. Semenova, M. M. Jore, K. A. Datsenko, A. Semenova, E. R. Westra, B. Wanner, van der J. Oost, S. J. J. Brouns, K. Severinov, *Proc. Natl. Acad. Sci.* **2011**, 108(25), 10098. <https://doi.org/10.1073/pnas.1104144108>
- [54] Y. Zheng, J. Li, B. Wang, J. Han, Y. Hao, S. Wang, X. Ma, S. Yang, L. Ma, L. Yi, W. Peng, *Front. Bioeng. Biotechnol.* **2020**, 8, 62. <https://doi.org/10.3389/fbioe.2020.00062>
- [55] H. Ledford, E. Callaway, *Nature* **2020**, 586(7829), -347.
- [56] H. Hirano, J. S. Gootenberg, T. Horii, O. O. Abudayyeh, M. Kimura, P. D. Hsu, T. Nakane, R. Ishitani, I. Hatada, F. Zhang, H. Nishimasu, O. Nureki, *Cell* **2016**, 164(5), 950. <https://doi.org/10.1016/j.cell.2016.01.039>
- [57] M. Azhar, R. Phutela, A. H. Ansari, D. Sinha, N. Sharma, M. Kumar, M. Aich, S. Sharma, R. Rauthan, K. Singhal, H. Lad, P. K. Patra, G. Makharia, G. R. Chandak, D. Chakraborty, S. Maiti, *bioRxiv* **2021**, 183, 113207. <https://doi.org/10.1016/j.bios.2021.113207>
- [58] S. Arnimesh, *The Print*, May 7, **2020**.
- [59] PIB DELHI, *Ministry of Science & Technology*, September 19, **2020**.
- [60] Health Desk, *IndiaTV News*, November 20, **2020**.
- [61] A. Pacha, *The Hindu* October 12, **2020**.
- [62] M.ohd Azhar, R. Phutela, M. Kumar, A. H. Ansari, R. Rauthan, S. Gulati, N. Sharma, D. Sinha, S. Sharma, S. Singh, S. Acharya, S. Sarkar, D. Paul, P. Kathpalia, M. Aich, P. Sehgal, G. Ranjan, R. C. Bhojar, K. Singhal, H. Lad, P. K. Patra, G. Makharia, G. R. Chandak, B. Pesala, D. Chakraborty, S. Maiti, *Biosens. Bioelectron.* **2021**, 183, 113207. <https://doi.org/10.1016/j.bios.2021.113207>
- [63] M. S. Draz, H. Shafiee, *Theranostics* **2018**, 8(7), 1985. <https://doi.org/10.7150/thno.23856>
- [64] M. Jauset-Rubio, M. Svobodová, T. Mairal, C. McNeil, N. Keegan, A. Saeed, M. N. Abbas, M. S. El-Shahawi, A. S. Bashammakh, A. O. Alyoubi, C. K. O'Sullivan, *Sci. Rep.* **2016**, 6(1), 37732. <https://doi.org/10.1038/srep37732>
- [65] ET Health World, *ETHealthworld.Com*. September 29, **2020**.
- [66] Y. Zhao, F. Chen, Q. Li, L. Wang, C. Fan, *Chem. Rev.* **2015**, 115(22), 12491. <https://doi.org/10.1021/acs.chemrev.5b00428>
- [67] M. Kumar, S. Gulati, A. Hussain Ansari, R. Phutela, S. Acharya, P. Kathpalia, A. Kanakan, R. Maurya, J. Srinivasa Vasudevan, A. Murali, R. Pandey, S. Maiti, D. Chakraborty, *eLife* **2021**, 10, e67130. <https://doi.org/10.7554/eLife.67130>

- [68] R. Aman, A. Mahas, M. Mahfouz, *ACS Synth. Biol.* **2020**, *9*(6), 1226. <https://doi.org/10.1021/acssynbio.9b00507>
- [69] Y. Li, S. Li, J. Wang, G. Liu, *Trends Biotechnol.* **2019**, *37*(7), 730. <https://doi.org/10.1016/j.tibtech.2018.12.005>
- [70] L. Li, S. Li, N. Wu, J. Wu, G. Wang, G. Zhao, J. Wang, *ACS Synth. Biol.* **2019**, *8*(10), 2228. <https://doi.org/10.1021/acssynbio.9b00209>
- [71] S.-Y. Li, Q.-X. Cheng, J.-M. Wang, X.-Y. Li, Z.-L. Zhang, S. Gao, R.-B. Cao, G.-P. Zhao, J. Wang, *Cell Discov.* **2018**, *4*(1), 20. <https://doi.org/10.1038/s41421-018-0028-z>
- [72] C. Escalona-Noguero, M. López-Valls, B. Sot, *BioEssays* **2021**, *43*(4), 2000315. <https://doi.org/10.1002/bies.202000315>
- [73] O. Piepenburg, C. H. Williams, D. L. Stemple, N. A. Armes, *PLoS Biol.* **2006**, *4*(7), 204. <https://doi.org/10.1371/journal.pbio.0040204>
- [74] T. Notomi, H. Okayama, H. Masubuchi, T. Yonekawa, K. Watanabe, K. Amino, T. Hase, *Nucleic Acids Res.* **2000**, *28*(12), e63. <https://doi.org/10.1093/nar/28.12.e63>
- [75] D. Thompson, Y. Lei, *Sens. Actuat. Rep.* **2020**, *2*(1), 100017. <https://doi.org/10.1016/j.snr.2020.100017>
- [76] S. Fu, G. Qu, S. Guo, L. Ma, N. Zhang, S. Zhang, S. Gao, Z. Shen, *Appl. Biochem. Biotechnol.* **2011**, *163*(7), 845. <https://doi.org/10.1007/s12010-010-9088-8>
- [77] Y. Kurosaki, N. Magassouba, O. K. Oloniyi, M. S. Cherif, S. Sakabe, A. Takada, K. Hirayama, J. Yasuda, *PLoS Negl. Trop. Dis.* **2016**, *10*(2), e0004472. <https://doi.org/10.1371/journal.pntd.0004472>
- [78] H. T. C. Thai, M. Q. Le, C. D. Vuong, M. Parida, H. Minekawa, T. Notomi, F. Hasebe, K. Morita, *J. Clin. Microbiol.* **2004**, *42*(5), 1956. <https://doi.org/10.1128/JCM.42.5.1956-1961.2004>
- [79] R. Nouri, Y. Jiang, X. L. Lian, W. Guan, *ACS Sens.* **2020**, *5*(5), 1273. <https://doi.org/10.1021/acssensors.0c00497>
- [80] F. Teng, L. Guo, T. Cui, X.-G. Wang, K. Xu, Q. Gao, Q. Zhou, W. Li, *Genome Biol.* **2019**, *20*(1), 1. <https://doi.org/10.1186/s13059-019-1742-z>
- [81] M. Kellner, J. Ross, J. Schnabl, M. Dekens, R. Heinen, I. Grishkovskaya, B. Bauer, J. Stadlmann, L. Menéndez-Arias, R. Fritsche-Polanz, M. Traugott, T. Seitz, A. Zoufaly, M. Födinger, C. Wensch, J. Zuber, A. Pauli, J. Brennecke, *bioRxiv* **2020**, <https://doi.org/10.1101/2020.06.23.166397>
- [82] P. R. Sahoo, K. Sathy, S. Mohapatra, D. Panda, *Vet. World* **2016**, *9*(5), 465. <https://doi.org/10.14202/vetworld.2016.465-469>
- [83] H. Shibata, A. Ogawa, N. Kanayama, T. Takarada, M. Maeda, *Anal. Chem.* **2013**, *85*(11), 5347. <https://doi.org/10.1021/ac400900b>
- [84] R. Nouri, Z. Tang, M. Dong, T. Liu, A. Kshirsagar, W. Guan, *Biosens. Bioelectron.* **2021**, *178*, 178. <https://doi.org/10.1016/j.bios.2021.113012>
- [85] X. Ding, K. Yin, Z. Li, R. V. Lalla, E. Ballesteros, M. M. Sfeir, C. Liu, *Nat. Commun.* **2020**, *11*(1), 1. <https://doi.org/10.1038/s41467-020-18575-6>
- [86] P. Chen, J. Zhou, Y. Wan, H. Liu, Y. Li, Z. Liu, H. Wang, J. Lei, K. Zhao, Y. Zhang, Y. Wang, X. Zhang, L. Yin, *Genome Biol.* **2020**, *21*(1), 78. <https://doi.org/10.1186/s13059-020-01989-2>
- [87] M. J. Kellner, J. G. Koob, J. S. Gootenberg, O. O. Abudayyeh, F. Zhang, *Nat. Protoc.* **2019**, *14*(10), 2986. <https://doi.org/10.1038/s41596-019-0210-2>
- [88] S. Shmakov, O. O. Abudayyeh, K. S. Makarova, Y. I. Wolf, J. S. Gootenberg, E. Semenova, L. Minakhin, J. Joung, S. Konermann, K. Severinov, F. Zhang, E. V. Koonin, *Mol. Cell* **2015**, *60*(3), 385. <https://doi.org/10.1016/j.molcel.2015.10.008>
- [89] J. P. Broughton, X. Deng, G. Yu, C. L. Fasching, V. Servellita, J. Singh, X. Miao, J. A. Streithorst, A. Granados, A. Sotomayor-Gonzalez, K. Zorn, A. Gopez, E. Hsu, W. Gu, S. Miller, C.-Y. Pan, H. Guevara, D. A. Wadford, J. S. Chen, C. Y. Chiu, *Nat. Biotechnol.* **2020**, *38*(7), 870. <https://doi.org/10.1038/s41587-020-0513-4>
- [90] J. Joung, A. Ladha, M. Saito, M. Segel, R. Bruneau, M. L. W. Huang, N. G. Kim, X. Yu, J. Li, B. D. Walker, A. L. Greninger, K. R. Jerome, J. S. Gootenberg, O. O. Abudayyeh, F. Zhang, *medRxiv* **2020**, <https://doi.org/10.1101/2020.05.04.20091231>
- [91] Z. Huang, D. Tian, Y. Liu, Z. Lin, C. J. Lyon, W. Lai, D. Fusco, A. Drouin, X. Yin, T. Hu, B. Ning, *Biosens. Bioelectron.* **2020**, *164*, 112316. <https://doi.org/10.1016/j.bios.2020.112316>
- [92] X. Ding, K. Yin, Z. Li, C. Liu, *bioRxiv* **2020**, <https://doi.org/10.1101/2020.03.19.998724>
- [93] X. Wang, M. Zhong, Y. Liu, P. Ma, L. Dang, Q. Meng, W. Wan, X. Ma, J. Liu, G. Yang, Z. Yang, X. Huang, M. Liu, *Sci. Bull.* **2020**, *65*(17), 1436. <https://doi.org/10.1016/j.scib.2020.04.041>
- [94] A. East-Seletsky, M. R. O'Connell, S. C. Knight, D. Burstein, J. H. D. Cate, R. Tjian, J. A. Doudna, *Nature* **2016**, *538*(7624), 270. <https://doi.org/10.1038/nature19802>
- [95] W. X. Yan, S. Chong, H. Zhang, K. S. Makarova, E. V. Koonin, D. R. Cheng, D. A. Scott, *Mol. Cell* **2018**, *70*(2), 327. <https://doi.org/10.1016/j.molcel.2018.02.028>
- [96] D. B. T. Cox, J. S. Gootenberg, O. O. Abudayyeh, B. Franklin, M. J. Kellner, J. Joung, F. Zhang, *Science* **2017**, *358*(6366), 1019. <https://doi.org/10.1126/science.aag0180>
- [97] O. O. Abudayyeh, J. S. Gootenberg, P. Essletzbichler, S. Han, J. Joung, J. J. Belanto, V. Verdine, D. B. T. Cox, M. J. Kellner, A. Regev, E. S. Lander, D. F. Voytas, A. Y. Ting, F. Zhang, *Nature* **2017**, *550*(7675), 280. <https://doi.org/10.1038/nature24049>
- [98] C. Zhang, S. Konermann, N. J. Brideau, P. Lotfy, X. Wu, S. J. Novick, T. Strutzenberg, P. R. Griffin, P. D. Hsu, D. Lyumkis, *Cell* **2018**, *175*(1), 212. <https://doi.org/10.1016/j.cell.2018.09.001>
- [99] J. S. Gootenberg, O. O. Abudayyeh, J. W. Lee, P. Essletzbichler, A. J. Dy, J. Joung, V. Verdine, N. Donghia, N. M. Daringer, C. A. Freije, C. Myhrvold, R. P. Bhattacharyya, J. Livny, A. Regev, E. V. Koonin, D. T. Hung, P. C. Sabeti, J. J. Collins, F. Zhang, *Science* **2017**, *356*(6336), 438. <https://doi.org/10.1126/science.aam9321>
- [100] S. Konermann, P. Lotfy, N. J. Brideau, J. Oki, M. N. Shokhiev, P. D. Hsu, *Cell* **2018**, *173*(3), 665. <https://doi.org/10.1016/j.cell.2018.02.033>
- [101] L. Liu, X. Li, J. Wang, M. Wang, P. Chen, M. Yin, J. Li, G. Sheng, Y. Wang, *Cell* **2017**, *168*(1-2), 121. <https://doi.org/10.1016/j.cell.2016.12.031>
- [102] L. Liu, X. Li, J. Ma, Z. Li, L. You, J. Wang, M. Wang, X. Zhang, Y. Wang, *Cell* **2017**, *170*(4), 714. <https://doi.org/10.1016/j.cell.2017.06.050>
- [103] C. Myhrvold, C. A. Freije, J. S. Gootenberg, O. O. Abudayyeh, H. C. Metsky, A. F. Durbin, M. J. Kellner, A. L. Tan, L. M. Paul, L. A. Parham, K. F. Garcia, K. G. Barnes, B. Chak, A. Mondini, M. L. Nogueira, S. Isern, S. F. Michael, I. Lorenzana, N. L. Yozwiak, B. L. MacInnis, I. Bosch, L. Gehrke, F. Zhang, P. C. Sabeti, *Science* **2018**, *360*(6387), 444. <https://doi.org/10.1126/science.aas8836>
- [104] J. S. Gootenberg, O. O. Abudayyeh, M. J. Kellner, J. Joung, J. J. Collins, F. Zhang, *Science* **2018**, *360*(6387), 439. <https://doi.org/10.1126/science.aag0179>
- [105] M. Patchsung, K. Jantarug, A. Pattama, K. Aphicho, S. Suraritdechachai, P. Meesawat, K. Sappakhaw, N. Leelahakorn, T. Ruenkam, T. Wongsatit, N. Athipanyasilp, B. Eiamthong, B. Lakkansirorot, T. Phoodokmai, N. Niljianskul, D. Pakotiprapha, S. Chanarat, A. Homchan, R. Tinikul, P. Kamutira, K. Phiwkaow, S. Soithongcharoen, C. Kantiwiryawanitch, V. Pongsupasa, D. Trisrivirat, J. Jaroensuk, T. Wongnate, S. Maenpuen, P. Chaiyen, S. Kamnerdnakta, J. Swangsri, S. Chuthapisith, Y. Sirivatanauksorn, C. Chaimayo, R. Suthent, W. Kantakamalakul, J. Joung, A. Ladha, X. Jin, J. S. Gootenberg, O. O. Abudayyeh, F. Zhang, N. Horthongkham, C. Uttamapinant, *Nat. Biomed. Eng.* **2020**, *4*(12), 1140. <https://doi.org/10.1038/s41551-020-00603-x>

- [106] J. Joung, A. Ladha, M. Saito, N.-G. Kim, A. E. Woolley, M. Segel, R. P. J. Barretto, A. Ranu, R. K. Macrae, G. Faure, E. I. Ioannidi, R. N. Krajeski, R. Bruneau, M.-L.W. Huang, X. G. Yu, J. Z. Li, B. D. Walker, D. T. Hung, A. L. Greninger, K. R. Jerome, J. S. Gootenberg, O. O. Abudayyeh, F. Zhang, *N. Engl. J. Med.* **2020**, 383(15), 1492. <https://doi.org/10.1056/NEJMc2026172>
- [107] J. Arizti-Sanz, C. A. Freije, A. C. Stanton, B. A. Petros, C. K. Boehm, S. Siddiqui, B. M. Shaw, G. Adams, T.-S.F. Kosoko-Thoroddsen, M. E. Kembball, J. N. Uwanibe, F. V. Ajogbasile, P. E. Eromon, R. Gross, L. Wronka, K. Caviness, L. E. Hensley, N. H. Bergman, B. L. MacInnis, C. T. Happi, J. E. Lemieux, P. C. Sabeti, C. Myhrvold, *Nat. Commun.* **2020**, 11(1), 5921. <https://doi.org/10.1038/s41467-020-19097-x>
- [108] J. N. Rauch, E. Valois, S. C. Solley, F. Braig, R. S. Lach, M. Audouard, J. C. Ponce-Rojas, M. S. Costello, N. J. Baxter, K. S. Kosik, C. Arias, D. Acosta-Alvarez, M. Z. Wilson, *J. Clin. Microbiol.* **2021**, 59(4), e02402. <https://doi.org/10.1128/JCM.02402-20>
- [109] D. J. Brogan, D. Chaverra-Rodriguez, C. P. Lin, A. L. Smidler, T. Yang, L. M. Alcantara, I. Antoshechkin, J. Liu, R. R. Raban, P. Belda-Ferre, R. Knight, E. A. Komives, O. S. Akbari, *medRxiv* **2020**, <https://doi.org/10.1101/2020.10.14.20212795>
- [110] C. M. Ackerman, C. Myhrvold, S. G. Thakku, C. A. Freije, H. C. Metsky, D. K. Yang, S. H. Ye, C. K. Boehm, T.-S.F. Kosoko-Thoroddsen, J. Kehe, T. G. Nguyen, A. Carter, A. Kulesa, J. R. Barnes, V. G. Dugan, D. T. Hung, P. C. Blainey, P. C. Sabeti, *Nature* **2020**, 582(7811), 277. <https://doi.org/10.1038/s41586-020-2279-8>
- [111] D. S. Mota, J. M. Marques, J. M. Guimarães, L. A. M. Mariúba, *Genet. Mol. Res.* **2020**, 19(1), <https://doi.org/10.4238/gmr18478>
- [112] C. A. Lino, J. C. Harper, J. P. Carney, J. A. Timlin, *Drug Deliv.* **2018**, 25(1), 1234. <https://doi.org/10.1080/10717544.2018.1474964>
- [113] T. R. Abbott, G. Dhamdhere, Y. Liu, X. Lin, L. Goudy, L. Zeng, A. Chemparathy, S. Chmura, N. S. Heaton, R. Debs, T. Pande, D. Endy, M. F. la Russa, D. B. Lewis, L. S. Qi, *Cell* **2020**, 181(4), 865. <https://doi.org/10.1016/j.cell.2020.04.020>
- [114] T. M. Nguyen, Y. Zhang, P. P. Pandolfi, *Cell Res.* **2020**, 30(3), 189. <https://doi.org/10.1038/s41422-020-0290-0>
- [115] D. Wilbie, J. Walther, E. Mastrobattista, *Acc. Chem. Res.* **2019**, 52(6), 1555. <https://doi.org/10.1021/acs.accounts.9b00106>
- [116] L. Buonaguro, M. Tagliamonte, M. L. Tornesello, F. M. Buonaguro, *J. Transl. Med.* **2020**, 18(1), 185. <https://doi.org/10.1186/s12967-020-02355-3>
- [117] J. S. Chen, E. Ma, L. B. Harrington, M. da Costa, X. Tian, J. M. Palefsky, J. A. Doudna, *Science* **2018**, 360(6387), 436. <https://doi.org/10.1126/science.aar6245>
- [118] K. Pardee, A. A. Green, M. K. Takahashi, D. Braff, G. Lambert, J. W. Lee, T. Ferrante, D. Ma, N. Donghia, M. Fan, N. M. Daringer, I. Bosch, D. M. Dudley, D. H. O'Connor, L. Gehrke, J. J. Collins, *Cell* **2016**, 165(5), 1255. <https://doi.org/10.1016/j.cell.2016.04.059>
- [119] D. S. Chertow, *Science* **2018**, 360(6387), 381. <https://doi.org/10.1126/science.aat4982>
- [120] F. Jia, X. Li, C. Zhang, X. Tang, *Protein Cell* **2020**, 11(9), 624. <https://doi.org/10.1007/s13238-020-00708-8>
- [121] A. Niu, A. McDougal, B. Ning, F. Safa, A. Luk, D. M. Mushatt, A. Nachabe, K. J. Zvezdaryk, J. Robinson, T. Peterson, F. Socola, H. Safah, T. Hu, N. S. Saba, *Bone Marrow Transplant.* **2020**, 55(12), 2354. <https://doi.org/10.1038/s41409-020-0972-8>
- [122] T. Hou, W. Zeng, M. Yang, W. Chen, L. Ren, J. Ai, J. Wu, Y. Liao, X. Gou, Y. Li, X. Wang, H. Su, B. Gu, J. Wang, T. Xu, *PLoS Pathog.* **2020**, 16(8), e1008705. <https://doi.org/10.1371/journal.ppat.1008705>
- [123] B. W. Buchan, J. S. Hoff, C. G. Gmehlin, A. Perez, M. L. Faron, L. S. Munoz-Price, N. A. Ledebner, *Am. J. Clin. Pathol.* **2020**, 154(4), 479. <https://doi.org/10.1093/ajcp/aqaa133>

How to cite this article: M. K. Verma, S. Roychowdhury, B. D. Sahu, A. Mishra, K. K. Sethi, *J. Biochem. Mol. Toxicol.* **2022**;36:e23113. <https://doi.org/10.1002/jbt.23113>